

Modelling techniques of ultrasonic wave propagation in solids

V. Daniulaitis, R. Barauskas

*Kaunas University of Technology, Department of Engineering Mechanics
Mickevièiaus 37, 3000 Kaunas, Lithuania*

Introduction

The range of ultrasonic applications in non-destructive testing and geometric measurements are of widespread use today as they provide simultaneously the versatility, non-destructive nature, reasonable amounts of information and are of a comparatively low price in comparison with other alternative methods. By virtue, the ultrasonic measurements in solids and composite bodies of a complicated geometrical shape often require to develop the case oriented equipment and image processing software basing upon the knowledge of the physical essence of the wave propagation in the environment under investigation. As a powerful tool for modelling of the ultrasonic measurement process the finite element method (FEM) can be used. The modelling of the ultrasonic wave propagation can be considered as the general small displacement transient structural dynamic problem, the solution techniques of which has been perfectly described in the early 1980 by numerous researchers [2, 1] and implemented today in practically all the FEM software available on the market. On the same mathematical base the ultrasonic application oriented finite element models [4, 5] have been made.

However, the practical application of such techniques is not always easy and efficient. As a rule, it requires highly refined meshes for proper presentation of the field of strains and displacements taking place in a body, the dimensions of which are of considerably larger than the length of the elastic wave propagating in a body. In this way even simple academic problems often require huge amounts of computational resources and for many practical applications the real price of the finite element modelling is prohibitive. In practice, sometimes the simplified analysis can be performed by means of a purely geometrical description of the wave pulse propagation and refraction from the walls of the body [5]. However, such an approach cannot be considered as physical modelling of the process, as it usually fails to present adequately the real strain-displacement field in the whole region. Moreover, actually it is not based upon the differential equations of vibrations of the solid body.

Only very few studies can be found in the literature coping directly with the problem of making the reasonable computational models that adequately describe the short wave propagation despite of the widespread range of possible applications. The same techniques would provide a powerful tool for modelling the vibroageing processes, the audio-frequency vibration propagation in very large structures such as ships, etc. On the contrary, practical all the effort up to now has been made for creating effective

models and techniques for structures vibrating in the frequency range of the lower modes.

This study presents the formulation of the possible ways of solution of the short wavelength transient vibration propagation in solid regions illustrated by simplest examples and evaluations of the effectivity of the approach.

Problem formulation

The motivation of the work is to find ways for effective numerical simulation small wavelength transient vibrations in solids. The efficiency of the method is understood as its speed and accuracy by using moderate computational recourses. A solid body is considered as the body the material properties of which (Young's modulus, density, Poisson's ratio) are close to metals. The wavelength of interest is defined basing on the ratio of the wave length to dimensions of the body and might be 1/1000 and even more.

The finite element method is widely used in order to examine structures in the case of static and dynamic loading. As a result, it provides the spatial discretization of the region in the form of the dynamic equations of the structure

$$[M]\{\ddot{U}\} + [K]\{U\} = \{F\} \quad (1)$$

where $[M]$, $[K]$ are the mass and stiffness matrices; $\{F\}$ is the external load vector; and $\{U\}$, $\{\ddot{U}\}$ are the nodal displacement and acceleration vectors of the structure. Damping term in (1) is being neglected.

The direct numerical integration techniques are used for the solution of the dynamic equation (1). The solution of the equilibrium equations always involves the approximation errors caused by time and space discretization. Practically, depending upon the selected numerical integration scheme, the limit of minimum 10 elements per wave length should be held in order to ensure the convergence of the solution. The step in time should be chosen properly either and varies from 10 to 20 steps per wave period. Finally, the number of the degrees of freedom of the structure and number of time steps n for solution required become very large for short wave problems. Moreover, the wave pulses or packages always contain quite wide spectra of harmonic components the higher part of which is inevitably distorted because for them the finite element mesh appears to be too rough. This can be seen from the example presented in Fig. 1 which illustrates the results when finite element per wave length was assumed.

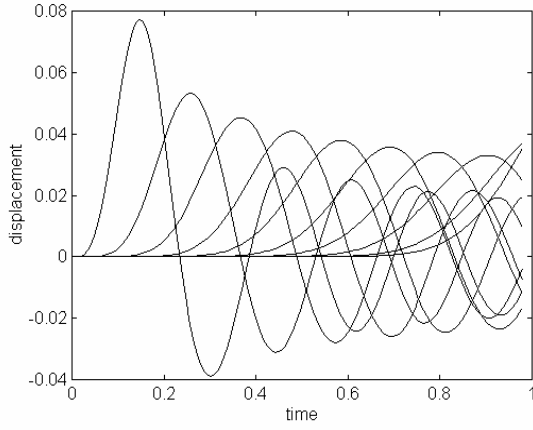


Fig. 1 Displacements of the nodes. One *sin*-shaped force pulse was assumed.

The amplitude of the wave pulse straightly decreases due to errors induced by the integration scheme. The reason is that the rough finite element mesh generates the refraction of the wave from the nodes of the model.

The results of two dimensional wave propagation analysis made by finite element system ANSYS show the fictitious waves that are being generated because the roughness of the model.

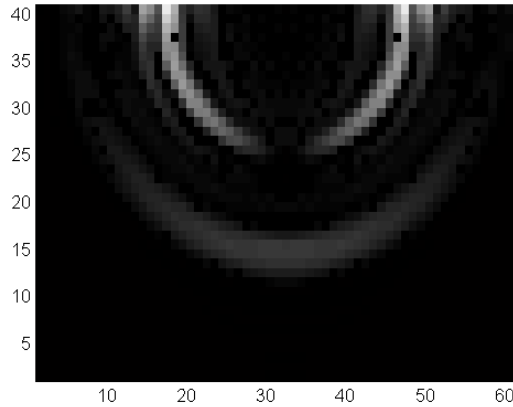


Fig. 2 Wave pulse propagation. One pulse of *sin*-shaped force, concentrated at the point was assumed.

To our point of view, the basic ways for coping with the above mentioned problem can be formulated as follows:

- employing the modified mass matrices of the element giving the minimum error while modelling the deformation pulse propagation in the body (it can be shown that neither lumped nor consistent types of the mass matrix are the optimum for such a problem);

- using dynamic substructures oriented for proper presentation of higher modal behaviour. This technique is well-known for computation in the range of lower natural frequencies;

- employing explicit numerical integration techniques and uniform meshes enabling to develop fast time stepping algorithms and in such a way to reduce the amounts of computation;

- employing models obtained by alternative methods, e.g., boundary integrals or finite difference methods for spatial discretization.

This study deals only with the first and the last ways of treatment of the problem.

Modified mass matrices

Consider the dynamic equation of the finite element of an elastic rod presented as

$$\frac{\rho A l}{3} \begin{bmatrix} 1 & \frac{1}{2} \\ \frac{1}{2} & 1 \end{bmatrix} \begin{Bmatrix} \ddot{u}_1 \\ \ddot{u}_2 \end{Bmatrix} + \frac{EA}{l} \begin{bmatrix} 1 & -1 \\ -1 & 1 \end{bmatrix} \begin{Bmatrix} u_1 \\ u_2 \end{Bmatrix} = \begin{Bmatrix} F_1^e \\ F_2^e \end{Bmatrix} \quad (2)$$

where E, ρ are the modules of elasticity and density of the material, A, l are the cross sectional area and length of the element, F_1^e, F_2^e are the nodal forces presenting the interaction of the element with neighbouring elements and concentrated external nodal loads.

Equation (2) can be transformed to modal coordinates by obtaining the eigenfrequencies and eigenforms of the element from the following equation:

$$\det \begin{bmatrix} k & -k \\ -k & k \end{bmatrix} - \omega^2 \begin{bmatrix} m & \frac{m}{2} \\ \frac{m}{2} & m \end{bmatrix} = 0, \quad (3)$$

where $m = \frac{\rho A l}{3}, k = \frac{EA}{l}$.

Equation (2) presented in modal coordinates reads as

$$\begin{bmatrix} 1 & 0 \\ 0 & 1 \end{bmatrix} \begin{Bmatrix} \ddot{z}_1 \\ \ddot{z}_2 \end{Bmatrix} + \begin{bmatrix} 0 & 0 \\ 0 & \frac{4k}{m} \end{bmatrix} \begin{Bmatrix} z_1 \\ z_2 \end{Bmatrix} = [Y]^T \begin{Bmatrix} F_1^e \\ F_2^e \end{Bmatrix} \quad (4)$$

where z_1, z_2 are the generalised displacement of the element related to the displacements

u_1, u_2 as $\begin{Bmatrix} u_1 \\ u_2 \end{Bmatrix} = [Y] \begin{Bmatrix} z_1 \\ z_2 \end{Bmatrix}, [Y] = \begin{bmatrix} \frac{1}{\sqrt{3m}} & \frac{1}{\sqrt{m}} \\ \frac{1}{\sqrt{3m}} & -\frac{1}{\sqrt{m}} \end{bmatrix}$ - matrix

of normalised eigenvectors satisfying the relation $[Y]^T [M] [Y] = [I]$.

Now we apply the approach widely used in dynamic reduction of structural equations the essence of which is the truncation of the dynamic contribution of the modes selected.

By truncating the dynamic contribution of the higher mode we obtain:

$$\begin{bmatrix} 1 & 0 \\ 0 & 0 \end{bmatrix} \begin{Bmatrix} \ddot{z}_1 \\ \ddot{z}_2 \end{Bmatrix} + \begin{bmatrix} 0 & 0 \\ 0 & \frac{4k}{m} \end{bmatrix} \begin{Bmatrix} z_1 \\ z_2 \end{Bmatrix} = [Y]^T \begin{Bmatrix} F_1^e \\ F_2^e \end{Bmatrix}; \quad (5.1)$$

and by truncating the dynamic contribution of the lower one we obtain:

$$\begin{bmatrix} 0 & 0 \\ 0 & 1 \end{bmatrix} \begin{Bmatrix} \ddot{z}_1 \\ \ddot{z}_2 \end{Bmatrix} + \begin{bmatrix} 0 & 0 \\ 0 & \frac{4k}{m} \end{bmatrix} \begin{Bmatrix} z_1 \\ z_2 \end{Bmatrix} = [Y]^T \begin{Bmatrix} F_1^e \\ F_2^e \end{Bmatrix}. \quad (5.2)$$

Now we shall write equations (5.1), (5.2) by using the original displacements u_1, u_2 as unknowns:

$$\frac{3m}{4} \begin{bmatrix} 1 & 1 \\ 1 & 1 \end{bmatrix} \begin{Bmatrix} \ddot{u}_1 \\ \ddot{u}_2 \end{Bmatrix} + \begin{bmatrix} k & -k \\ -k & k \end{bmatrix} \begin{Bmatrix} u_1 \\ u_2 \end{Bmatrix} = \begin{Bmatrix} F_1^e \\ F_2^e \end{Bmatrix}; \quad (6.1)$$

$$\frac{m}{4} \begin{bmatrix} 1 & -1 \\ -1 & 1 \end{bmatrix} \begin{Bmatrix} \ddot{u}_1 \\ \ddot{u}_2 \end{Bmatrix} + \begin{bmatrix} k & -k \\ -k & k \end{bmatrix} \begin{Bmatrix} u_1 \\ u_2 \end{Bmatrix} = \begin{Bmatrix} F_1^e \\ F_2^e \end{Bmatrix}. \quad (6.2)$$

Equations (6.1) and (6.2) contain two alternatives of the mass matrix of the element

$$\left[M_l^e \right] = \frac{3m}{4} \begin{bmatrix} 1 & 1 \\ 1 & 1 \end{bmatrix}; \left[M_h^e \right] = \frac{m}{4} \begin{bmatrix} 1 & -1 \\ -1 & 1 \end{bmatrix},$$

corresponding to the reduced dynamic equations with truncated modal contributions of the higher and lower modes correspondingly. The sum of the two matrices equals the consistent mass matrix of the structure:

$$\left[M_l^e \right] + \left[M_h^e \right] = m \begin{bmatrix} 1 & \frac{1}{2} \\ \frac{1}{2} & 1 \end{bmatrix}. \quad (7)$$

By changing the contributions of the above mentioned components of the mass matrix and by retaining the total mass of the element unchanged, various expressions of the mass matrix of the element can be obtained. For example, by adding the components with the weight coefficients 1 and 3 gives the lumped mass matrix:

$$\left[M_l^e \right] + 3 \left[M_h^e \right] = \frac{3m}{2} \begin{bmatrix} 1 & 0 \\ 0 & 1 \end{bmatrix}. \quad (8)$$

It is obvious, that the coefficient at $\left[M_l^e \right]$ is always unity, as it controls the value of the mass of the element, and the coefficient at $\left[M_h^e \right]$ can be any number, as the total mass provided by $\left[M_h^e \right]$ is of zero value. By means of numerical experiments has been shown that the mass matrix obtained as

$$\left[M_l^e \right] + \frac{29}{16} \left[M_h^e \right] = \begin{bmatrix} \frac{77m}{64} & \frac{19m}{64} \\ \frac{19m}{64} & \frac{77m}{64} \end{bmatrix} \quad (9)$$

provides optimum accuracy by modelling the short wave propagation in the rod.

The following Fig. 3, Fig. 4, Fig. 5 represent the results when “consistent”, “lumped” and modified (9) mass matrices were assumed. The one *sin*-shaped force pulse with the length equal to five finite element lengths was applied to the structure.

Fig 6 represent the results when “lumped” mass matrix and finer element mesh, including 25 elements per wave length, and one *sin*-shaped force loading were assumed.

It is obvious that the “lumped” and “consistent” mass

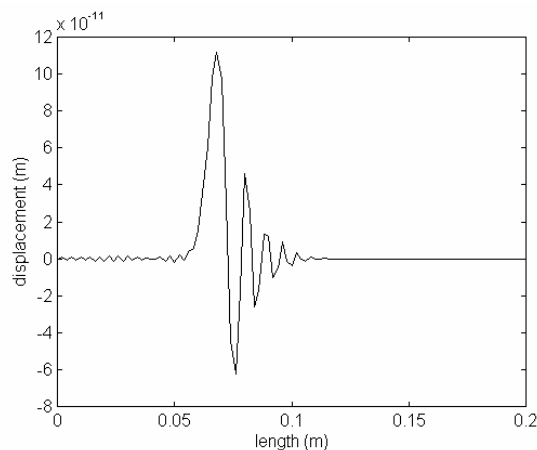


Fig. 3 The wave pulse propagation for “consistent” mass matrix.

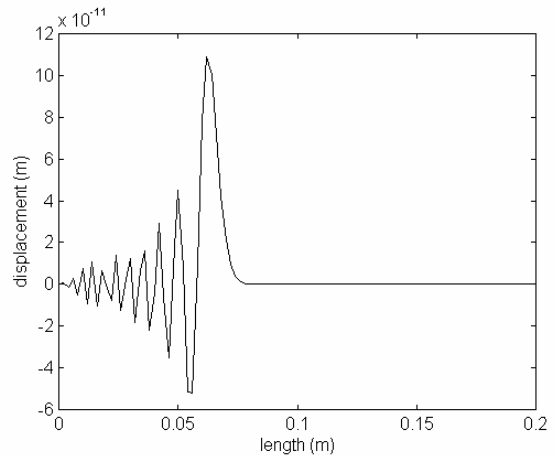


Fig. 4 The wave pulse propagation for “lumped” mass matrix.

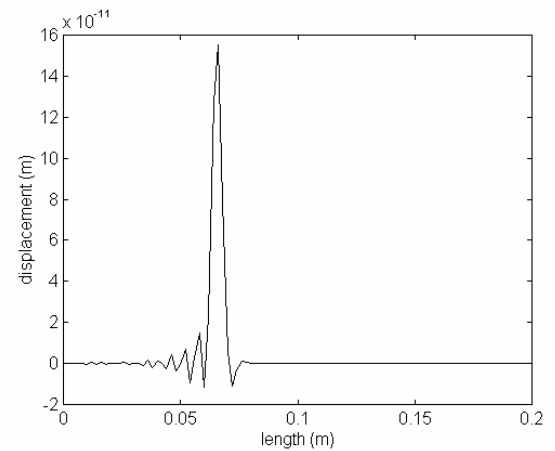


Fig. 5 The wave pulse propagation for modified mass matrix.

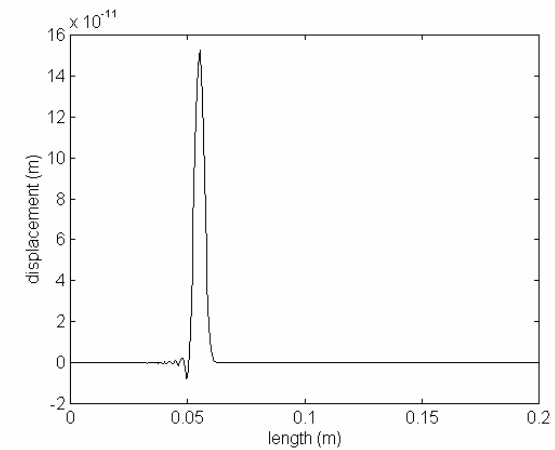


Fig. 6 The wave pulse propagation for “lumped” mass matrix.

matrices generates additional “noise” signal which is not negligible when small element number per wave length is assumed. Matrix modification enables to use the more rough element mesh and saves time for calculations required.

Boundary integral equation approach

The boundary element method was developed in the late fifties of the current century. At the time being the boundary element method is widely developed and often presents an alternative to the finite element method as it has the following advantages. First, only the boundary of the structure has to be meshed. Second, there is no need to define boundary conditions because they are naturally included into equations. Third, the method is recommended when modelling areas with a high stress concentration.

The displacement of any point of the elastic body in general is described as:

$$u_j(\xi) = \int_A [t_i(x)G_{ij}(x, \xi) - F_{ij}(x, \xi)u_i(x)]dA(x) + \int_V \psi_i(z)G_{ij}(z, \xi)dV(z), \quad (10)$$

where t_i are the loads on the boundary, $G_{ij}(x, \xi)$ is the Green's function, $F_{ij}(x, \xi)$ is the coordinate dependent derivative of the Green's function, $\psi_i(z)$ - body loads of the structure. Equation (10) describes displacements caused by the static load. In the case of unidimensional structure in absence of the body loads equation (10) reduces to

$$u_j(\xi, t) = [G_{ij}t_i - F_{ij}u_i]_0^L. \quad (11)$$

The Green's function G is given by:

$$G = \frac{1}{2c}H(ct - r), \quad (12)$$

where H is the Heaviside function:

$$H = \begin{cases} 1, & \text{when } (ct - r) > 0 \\ 0, & \text{when } (ct - r) < 0 \end{cases} \quad (13)$$

where r corresponds to the position vector, c is the wave velocity in the material.

F is obtained as

$$F = \frac{\partial G}{\partial n} = \frac{\partial}{\partial x} \frac{1}{2c} H(ct - r). \quad (14)$$

The dynamic equilibrium is examined by introducing in addition the time dimension and by carrying out the integration. The integration in time is performed by means of the convolution operation denoted by the sign “* “. The dynamic version of the equation (10) is given by:

$$u_j(\xi, t) = \int_A [G_{ij} * t_i - F_{ij} * u_i]dA(x) + \int_V \rho [G_{ij} * \psi_i]dV(x) + \int_V \rho \left[V_i'(x)G_{ij}(x, t; \xi, 0) + u_i'(x) \frac{\partial G_{ij}(x, t; \xi, 0)}{\partial t} \right]dV(x). \quad (15)$$

The last integral in (15) represents the initial conditions of the structure. When using zero initial conditions and examining the unidimensional structure, the dynamic version of (11) can be presented as:

$$u_j(\xi, t) = [G_{ij} * t_i - F_{ij} * u_i]_0^L. \quad (16)$$

The equation (16) includes the displacements and forces at both ends as unknowns. If the problem is formulated properly, two of them have to be prescribed and the remaining two can be obtained. Consider the

structure presented on Fig. 7, the loading of which is defined as:

$$t_{(a)} = t_{(0)} = \sin(\omega t); t_{(b)} = t_{(L)} = 0. \quad (17)$$

We write equation in the form (16) for the left-hand end (boundary element a), and the right-hand end (boundary element b) as

$$\begin{cases} u_{1(0)} = G_2 * t_{(L)} - G_1 t_{(0)} - F_2 * u_{(L)} + F_1 * u_{(0)} \\ u_{2(L)} = G_3 * t_{(L)} - G_4 t_{(0)} - F_3 * u_{(L)} + F_4 * u_{(0)} \end{cases}, \quad (18)$$

where subscripts (0) , (L) correspond to the loads and displacements at left- and right hand ends of the structure respectively. The indices 1, 2, 3, 4 represent the Green's

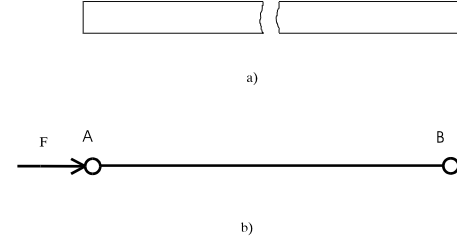


Fig. 7 Uniform rod (a), boundary element model (b).

functions and coordinate dependent derivatives of them obtained from equations (12) and (14).

Equations (18) can be presented in the matrix form as:

$$\begin{Bmatrix} u_{1(0)} \\ u_{2(L)} \end{Bmatrix} = \begin{bmatrix} G_2 & -G_1 \\ G_3 & -G_4 \end{bmatrix} * \begin{Bmatrix} t_{(L)} \\ t_{(0)} \end{Bmatrix} + \begin{bmatrix} -F_2 & F_1 \\ -F_3 & F_4 \end{bmatrix} * \begin{Bmatrix} u_{(L)} \\ u_{(0)} \end{Bmatrix}. \quad (19)$$

By representing the convolution operation by integrals and by splitting the second matrix term in the equation (19), we obtain:

$$\begin{Bmatrix} u_{1(0)} \\ u_{2(L)} \end{Bmatrix} = \int_0^{N\Delta\tau} \begin{bmatrix} G_2 & -G_1 \\ G_3 & -G_4 \end{bmatrix} \begin{Bmatrix} t_{(L)} \\ t_{(0)} \end{Bmatrix} d\tau + \int_0^{(N-1)\Delta\tau} \begin{bmatrix} -F_2 & F_1 \\ -F_3 & F_4 \end{bmatrix} \begin{Bmatrix} u_{(L)} \\ u_{(0)} \end{Bmatrix} d\tau + \int_{(N-1)\Delta\tau}^{N\Delta\tau} \begin{bmatrix} -F_2 & F_1 \\ -F_3 & F_4 \end{bmatrix} \begin{Bmatrix} u_{(L)} \\ u_{(0)} \end{Bmatrix} d\tau \quad (20)$$

where $N\Delta t$ indicates the current moment in the time discretization. The left side vector and the last term of the equations (20) represents the displacements at the current time step.

If the displacements $u_{(L)}$ and $u_{(0)}$ are assumed to be constant at the current time step, equations (20) may be rewritten as:

$$\begin{Bmatrix} u_{1(0)} \\ u_{2(L)} \end{Bmatrix} - \int_{(N-1)\Delta\tau}^{N\Delta\tau} \begin{bmatrix} -F_2 & F_1 \\ -F_3 & F_4 \end{bmatrix} \begin{Bmatrix} u_{(L)} \\ u_{(0)} \end{Bmatrix} d\tau = \int_0^{N\Delta\tau} \begin{bmatrix} G_2 & -G_1 \\ G_3 & -G_4 \end{bmatrix} \begin{Bmatrix} t_{(L)} \\ t_{(0)} \end{Bmatrix} d\tau + \int_0^{(N-1)\Delta\tau} \begin{bmatrix} -F_2 & F_1 \\ -F_3 & F_4 \end{bmatrix} \begin{Bmatrix} u_{(L)} \\ u_{(0)} \end{Bmatrix} d\tau. \quad (21)$$

After cancellation the equation system (21) reads as:

$$\begin{bmatrix} 1 - \int_{N\Delta\tau} F_1 d\tau & \int_{N\Delta\tau} F_2 d\tau \\ - \int_{N\Delta\tau} F_4 d\tau & 1 + \int_{N\Delta\tau} F_3 d\tau \end{bmatrix} \begin{Bmatrix} u_1(0) \\ u_2(L) \end{Bmatrix}^{N\Delta\tau} = \int_0^{N\Delta\tau} \begin{bmatrix} G_2 & -G_1 \\ G_3 & -G_4 \end{bmatrix} \begin{Bmatrix} t(L) \\ t(0) \end{Bmatrix} d\tau + \int_0^{(N-1)\Delta\tau} \begin{bmatrix} -F_2 & F_1 \\ -F_3 & F_4 \end{bmatrix} \begin{Bmatrix} u(L) \\ u(0) \end{Bmatrix} d\tau \quad (22)$$

The equation system (22) is linear with respect to the displacements $u(L)$, $u(0)$ and can be easily solved for the current time step from solutions at previous times considered.

The solution of the equations (22) is represented in Fig. 6.

The structure was subjected by one *sin*-shaped force pulse. The first pulse in Fig. 6 indicates the displacement of the boundary element *a*, the second pulse - the displacement of the element *b*, the third - displacement of the element *a* caused by the wave reflected from the element *b*. The fine wave pulses were calculated using boundary integral equation approach. Despite of the good results the boundary integral equation approach is time consuming. The perform of a convolution is the most time consuming operation. The efficiency of the algorithm can be improved by means of standard operations, using the fast convolution evaluation technique for example.

Conclusions

Two ways of the short wave propagation modelling in

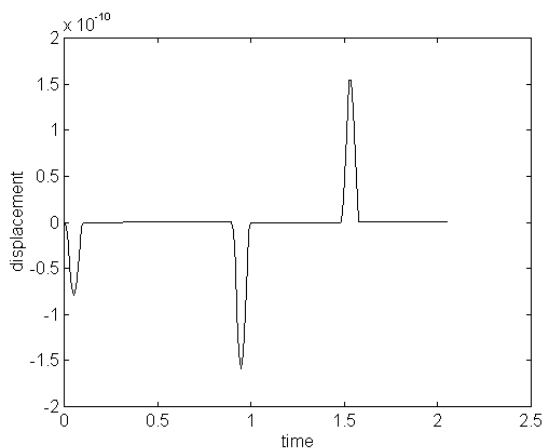


Fig.8 The wave pulse propagation.

a solid body were analysed. The experimental data confirms that the conventional modelling techniques as the finite element approach combined with the numerical integration for space and time discretization does not

simulate adequately the wave pulse propagation. The mass matrix modification method has been proposed based upon the dynamic reduction approach. It provides better results of the signal to noise ratio thus enabling to obtain the finer wave pulse by means of the model.

The boundary integral equation approach has been analysed as an alternative way to the finite element technique. The algorithm enables to obtain the noise-free signals by means of the model. Consequently, the calculated displacements are in good agreement with exact displacements. Despite of precision of the technique the calculations were time consuming in comparison with the finite element approach.

Acknowledgement

This work is supported in part by Lithuanian State Science and Studies foundation.

References

1. J. H. Argyris, J. St. Doltsinis, W. C. Knudson, L. E. Vaz, K. J. Willam. Numerical Solution of Transient Nonlinear Problems// Comp. Meths. Appl. Mech. Eng. - 1979. 17/18.- P. 341-409.
2. K. J. Bathe, E. L. Wilson. Numerical methods in finite element analysis// - PRENTICE-HALL, INC., Englewood Cliffs, New Jersey.
3. T. Belytschko. On difficulty levels in non linear finite element analysis of solids// Bulletin for the international association for computational mechanics.- 1996. No. 2.
4. Y. Kawaga, G. M. L. Gladwell. Finite Element Analysis of Flexure-Type Vibrators with Electrostrictive transducers// IEEE Trans. on Sonics and Ultrasonics.- 1970.- SU-17(1).-P. 41-50.
5. Л. Ю. Мажейка. Исследование и разработка измерительных пьезопреобразователей, работающих в нестационарном режиме, методом конечных элементов// Каунас, 1985.
6. К Бреббия, С. Уокер. Применение метода граничных элементов в технике// Москва: Мир.- 1982.-С. 248.
7. П. Бенерджи, Р. Батерфилд. Методы граничных элементов в прикладных науках// Москва: Мир.- 1984.-С.494.
8. А. Б. Васильева, Н. А. Тихонов. Интегральные уравнения// Москва: Издательство Московского университета.- 1989.- С.156.
9. Й. Крауткремер, Г. Крауткремер. Ультразвуковой контроль материалов// Москва: Металлургия.- 1991.-С. 750 .

V. Daniulaitis, R. Barauskas

Ultragarso bangų sklaidimo kietuose kūnuose modeliavimo metodai

Reziumė

Darbe nagrinėjami standžiam kūne sklindančių bangų, kurių ilgis gerokai mažesnis už kūno matmenis, kompiuterinio modeliavimo metodai. Tradicinis baigtinių elementų metodas gerai tinka banginiams procesams tirti, jeigu bangos ilgis yra tos pačios eilės kaip ir konstrukcijos matmenys. Trumpėjant bangai, sprendinys vis labiau iškraipomas, kadangi diskretinis modelis nepakankamai tiksliai aprašo aukštesias virpesių harmonikas. Darbe apžvelgti du būdai šiai problemai išspręsti: pasiūlytas elemento masių matricos modifikavimo metodas bei išnagrinėtos kraštinių integralinių lygčių metodo pritaikymo galimybės.